Large salp bloom export from the upper ocean and benthic community response in the abyssal northeast Pacific: day to week resolution

Authors:

K.L. Smith, Jr.[1], A.D. Sherman[1], C.L. Huffard[1], P.R. McGill[1], R. Henthorn[1], S. Von Thun[1], H.A. Ruhl[2], M. Kahru[3], M.D. Ohman[3]

[1] Monterey Bay Aquarium Research Institute, Moss Landing, California 95039

[2] National Oceanography Centre, Southampton, United Kingdom

[3] Scripps Institution of Oceanography, University of California, San Diego, California, 92093-0218

Running head: Salp bloom and abyssal response

Acknowledgments

This research was supported by the National Science Foundation and the David and Lucile Packard Foundation. We thank many of our colleagues over the many years of this time-series study including R. Baldwin, A. Uhlman, R. Wilson, J. Ellena, and the crews of R/V *New Horizon*, R/V *Atlantis* and R/V *Western Flyer*. The ROV Doc Ricketts pilots provided great support for our project. L. Kuhnz and L. Clary identified many of the benthic fauna and spent many hours digitizing time-lapse images. Holothurian voucher specimens were identified by A. Gebruk and A. Rogacheva. L. Sala and B. Lavaniegos identified the CalCOFI salps. This is a contribution from the NSF-supported California Current Ecosystem LTER site. The authors declare no conflicts of interest.

Abstract

A large bloom of *Salpa* spp. in the northeast Pacific during spring 2012 resulted in a major deposition of tunics and fecal pellets on the sea floor at ~4000 m depth (Sta. M) over a period of six months. Continuous monitoring of this food pulse was recorded using autonomous instruments: sequencing sediment traps, a time-lapse camera on the sea floor and a bottom-transiting vehicle measuring sediment community oxygen consumption (SCOC). These deep-sea measurements were complemented by sampling of salps in the epipelagic zone by California Cooperative Ocean Fisheries Investigations (CalCOFI). The particulate organic carbon (POC) flux increased sharply beginning in early March, reaching a peak of 38 mg C $m^{-2}d^{-1}$ in mid-April at 3400 m depth. Salp detritus started appearing in images of the sea floor taken in March, and covered a daily maximum of 98% of the sea floor from late June to early July. Concurrently the SCOC rose with increased salp deposition, reaching a high of 31 mg C $m^{-2}d^{-1}$ in late June. A dominant megafauna species, *Peniagone* sp. nov., increased 7-fold in density beginning seven weeks after the peak in salp deposition. Estimated food supply from salp detritus was 97 to 327% of the SCOC demand integrated over the six month period starting in March 2012. Such large episodic pulses of food sustain abyssal communities over extended periods of time.

Introduction

Episodic pulses of food reaching the deep-sea are extremely important in sustaining abyssal communities over long time periods. Long time-series measurements of particulate organic carbon (POC) flux into the deep-sea have revealed benthic community food shortages spanning two decades (Smith and Kaufmann 1999; Smith et al. 2009). However, short episodic pulses can quickly import enough food to sustain the benthic communities over long periods of deficit as revealed in a 24-year time series study in the northeast Pacific (Smith et al. in press).

The principal source of food for deep-sea communities is derived from primary production of organic matter in surface waters. Packaging of this organic matter, either as phytoplankton or from higher trophic level derivatives, is critical to the transfer of food to the abyssal sea floor. One group of upper-ocean gelatinous zooplankton, salps, are adept at effectively filtering large volumes of water, extracting phytoplankton and other particles as small as picoplankton, and having high defecation rates (Andersen 1998) of compact fecal pellets that sink rapidly. Salps can occur in large swarms or "blooms," which are induced by high filtration (feeding) rates, rapid growth, and alternation of sexual and asexual reproduction (Madin et al. 2006). Such salp swarms have been recorded over extensive areas, as great as 9065km^2, in many regions of the world ocean, including the northeastern Pacific (Berner 1967; Lavaniegos and Ohman 2003), southwestern Pacific (Henschke et al. 2013), northwestern Atlantic (Wiebe et al. 1979; Madin et al. 2006) and northeastern Atlantic (Bathmann 1988). These blooms have been observed to last from weeks to several months (Berner 1967; Andersen 1998).

Rapid sinking of salp fecal pellets and tunics effectively transports enriched organic matter into the deep ocean (Matsueda et al. 1986; Morris et al. 1988; Lebrato et al. 2013). Although salps have prolific feeding rates, much of the material in their fecal pellets can be

undigested phytoplankton with intact chloroplasts (Madin 1974; Silver and Bruland 1981; Harbison et al. 1986). Once on the sea floor, these salp products can serve as a food source for deep-sea benthic organisms (Wiebe et al. 1979; Pfannkuche and Lochte 1993; Henschke et al. 2013). To date, studies of salp bloom impacts on deep-sea ecosystems have shown an efficient downward transport mechanism of organic carbon toward the sea floor. However, to our knowledge previous studies have not monitored the magnitude of the salp flux reaching benthic communities, or longer term impacts of such food pulses on deep-sea processes. Here we present a multifaceted monitoring of a spring salp bloom as a food supply to the deep ocean, and its resulting impact on the benthic community, within the temporal context of a 24-year time series study of abyssal processes. We use these data to show how salps can provide an episodic but substantial mechanism of carbon transport from surface waters to abyssal depths, and that this food source can quickly elicit carbon mineralization by benthic communities.

Methods

This study was conducted at a long time-series station (Sta. M) in the northeast Pacific Ocean where measurements of deep-sea processes combined with atmospheric and surface ocean conditions have been monitored over the past 24 years. Waters overlying this abyssal site (~ 4000 m depth) show strong seasonal primary production corresponding to upwelling events within the California Current. Seasonal records of phytoplankton and zooplankton in the upper 210 m of this general area have been collected over the past 65 years [California Cooperative Ocean Fisheries Investigations (CalCOFI) program] (Ohman and Smith 1995). The continuous monitoring efforts at Sta. M were begun in 1989 with sediment traps moored at 3400 and 3950 m depth to collect sinking particulate matter as an estimate of food supply reaching the sea floor (Smith et al. 1994; Smith and Druffel 1998). Concurrently, a time-lapse camera at the bottom of

the mooring monitored hourly changes in sedimentation events and megafaunal movements over approximately 20 m^2 of the sea floor (Sherman and Smith 2009; Smith et al. 1993). Seasonal measurements of sediment community oxygen consumption (SCOC), as an estimate of organic carbon consumed, were made using a free vehicle grab respirometer (Smith 1987) until 2011, after which continuous measurements of SCOC were recorded using an autonomous bottom-transiting vehicle (Benthic Rover; (McGill et al. 2009; Sherman and Smith 2009). This dual-tracked vehicle transited the sea-floor stopping every ten m to make two-day measurements of SCOC. The Benthic Rover also took high-resolution images of the seafloor while transiting between measurement sites, providing monitoring of megafauna density and quantitative assessment of sedimentation events (155 transits, 1423 frames examined). A camera mounted obliquely, 112 cm above the sea floor, on the Benthic Rover frame provided clear images of salp tunics and phyto-detrital aggregates. The Benthic Rover is also equipped with a blue-light source and a camera utilizing a 675 nm low-pass filter (Henthorn et al. 2010) to document sediment-surface fluorescence that might result from chlorophyll excitation (McGill et al. 2009; Sherman and Smith 2009). When annotating Rover transit images to count megafauna, reference objects on the seafloor were used to determine a unique field of view for each frame, and prevent duplicate counts of the same individual in successive frames. Detailed descriptions of the methods used in this study are given below.

Satellite estimates of chlorophyll and net primary production:

We used regionally optimized algorithms (Kahru et al. 2012) based on satellite measurements from four ocean color sensors (OCTS, SeaWiFS, MODIS-Aqua and MERIS) to estimate near-surface chlorophyll-*a* concentration (Chl-*a*). A version of the Behrenfeld and Falkowski (1997) VGPM algorithm was applied to the satellite-derived Chl-a data from the

California Current region (Kahru et al. 2009) to estimate net primary production (NPP). Monthly mean values of all satellite-derived variables were averaged in a circle with a 100 km radius circle around Station M (Smith et al. 2006; Smith et al. 2008; Kahru et al. 2012).

Water column sampling for zooplankton: Mesozooplankton were sampled with a 71-cm, 505-µm mesh bongo net in the upper 210 m (Ohman and Smith 1995), or shallower depths, on the California Cooperative Oceanic Fisheries Investigations (CalCOFI) cruises. All salp zooids were enumerated by species from springtime CalCOFI cruises and converted to carbon biomass using the species-specific length-carbon relationships in Lavaniegos and Ohman (2007). For most cruises, individual samples were pooled prior to enumeration, according to the protocol in Lavaniegos and Ohman (2007). Spring 2012 samples were analysed individually and thus not pooled. Zooplankton displacement volume was determined as the "large" fraction (i.e. summed displacement volume of individual organisms > 5mL individual volume) and the "small" fraction (all remaining organisms). Displacement volume and salp carbon biomass are expressed as the total epipelagic biomass integrated under one m^2 of sea surface, from surface to 210 m depth.

POC flux:

Particulate organic carbon (POC) flux was measured from samples collected by sequencing sediment traps with a sampling resolution of ten days (Smith et al. 1994). Traps were moored at 50 and 600 meters above bottom (mab) respectively. From 1989-2010, sediment traps with a 13-sample cup sequencer were used, each with a Teflon-coated fiberglass funnel ($0.25m^2$ opening (Baldwin et al. 1998). From 2011–2012 we used 21-cup sediment traps (McLane Research Laboratories, Inc., p.n. PARFLUX Mark78H-21), each with a plastic funnel. The sediment trap opening was $0.5m^2$ and covered by a hexagonal-opening baffle (1.5 cm/side). Trap cups were filled with a poison prior to deployment (3.0 mM $HgCl_2$ from 1989-2009, 3%

buffered formalin from 2009-2012). Cups were examined immediately after recovery and zooplankton swimmers were removed. The remaining samples were frozen at -20°C. Salp fecal pellets and tunics were also counted in the sediment trap cups immediately after recovery but not removed from the sample. The organic carbon content of salp fecal pellets was estimated using 0.119 mg C $pellet^{-1}$ because pellet size was not measured (Wilson et al. 2013).

Samples were subsequently thawed, split, and ¾ of each sample analyzed for organic carbon content. This portion was freeze-dried, weighed and analyzed for total carbon in duplicate (Perkin-Elmer or Exeter Analytical elemental analyzer, University of California Santa Barbara Marine Science Institute Analytical Lab) and inorganic carbon (UIC coulometer). Because salt can represent a substantial portion of salp dry weight (Madin 1982) the samples were then corrected for salt content estimated from a $AgNO_3$ titration (Strickland and Parsons 1972). Salt content averaged 59 ± 3% s.d. of total dry weight. Salt-corrected inorganic carbon values were subtracted from salt-corrected total carbon to determine organic carbon. In order to obtain the most complete sediment trap record possible, we filled gaps in the 600 mab trap data with values from the 50 mab trap based on the linear regression $POC_{600\ MAB} = 3.2 + (0.44 \times POC_{50\ MAB})$. Of the 5841 total POC data points, 1045 were infilled using this method.

Water column and sea floor observations of salps and phytodetrital aggregates:

Two remotely operated vehicle (ROV) dives (402 and 403) were conducted at Sta. M in June 2012 with the ROV Doc Ricketts, from R/V *Western Flyer*. A high-definition video camera recorded the number of salps on descent to 4000 m and the subsequent ascent back to the surface on both dives, at constant speed (35 m min^{-1}).

A camera tripod at the base of the sediment trap mooring photo-documented the sea floor by taking one image every hour. A Canadian grid system (Wakefield and Genin 1987) was used

156 to estimate percent cover of detrital aggregates in daily images. Between 1989-2006 the tripod
157 was equipped with a film camera (Smith et al. 1993). A Graf/Bar Mark II digitizer was used to
158 determine the area coverage of individual aggregates in these images. Since 2007 the tripod has
159 been equipped with a digital camera of comparable image quality, as verified by overlapping
160 sampling (Sherman and Smith 2009). Individual detrital aggregate coverage of the sea floor in
161 digital images was determined using the Video Annotation and Reference System (VARS), an
162 open-source video annotation software (Schlining and Stout 2006), and a script that returns areas
163 within digitized outlines. Because the effective detection radius (EDR) for identifying detrital
164 aggregates varied between deployments according to water clarity, strobe illumination, and other
165 factors, we used the program Distance (Thomas et al. 2010) to calculate the EDR for each
166 deployment (version 2.1 for deployments in 2006 and prior, and version 4.1 for deployments
167 after 2006). EDR was then used to calculate effective area viewed. This program uses the radial
168 distance from a point in each detrital aggregate [center pixel of the small aggregates documented
169 from 1989 to 2006 (Smith et al. 2008), farthest pixel in the large aggregates documented from
170 2007 to 2012] to the bottom center pixel of each frame to fit a probability density function to the
171 observed distribution of aggregates. EDR as generated by Distance 4.1 was highly variable,
172 leading to variable effective viewed areas as well (13 to 32 m^2) and aggregate percent cover
173 exceeding 100% calculated for some frames. We applied a correction factor of 0.6061 to
174 aggregate percent cover values determined using Distance 4.1-generated EDR, thereby
175 referencing all frames against those with 100% coverage visible in original frames. Biases that
176 might be caused by this correction would cause an underestimate of aggregate organic carbon
177 flux from 2006 to 2012.
178 **SCOC measurements:**

Measurements of SCOC were obtained using a Free Vehicle Grab Respirometer (FVGR, (Smith 1987) and the Benthic Rover (Sherman and Smith 2009). Each instrument measured oxygen depletion during ~two-day-long incubations. The FVGR measured SCOC in the top 15 cm of sediment and overlying water using four grabs that each covered 413 cm^2 of seabed. The Benthic Rover transited across the seafloor's soft-substrate and stopped every ten m to make SCOC measurements within two acrylic chambers, each enclosing 730 cm^2 of sediment surface and overlying water. Cameras imaged each Benthic Rover chamber insertion depth into the seabed and allowed for identification of megafauna that might have been enclosed. An optode (Aanderaa, p.n. 3830) was used to measure dissolved oxygen depletion within each chamber and data were recorded for one minute every 15 minutes. A respiratory quotient of 0.85 was used to calculate sediment community carbon consumption rates based on rates measured by the FVGR and Benthic Rover (Smith 1987).

In November 2011 near-concurrent Benthic Rover and FVGR deployments allowed us to compare SCOC sampling methods. The values measured by the four FVGR chambers during one deployment, and the two Benthic Rover chambers over a period of ten days nearest the FVGR deployment date, overlapped with averages of 12.3 (+/- 0.1 standard deviation) and 12.24 (+/- 1.2 standard deviation) mg C m^{-2} d^{-1} respectively. This result demonstrates these two instruments provide similar estimates (Smith et al. in press). An earlier comparison between the FVGR and an older model of Benthic Rover also found that they yielded similar measures of SCOC (Smith et al. 1997).

Megafauna density:

Holothurian megafauna were identified to the lowest possible taxon and counted in daily camera tripod images. A voucher specimen and high definition video of this undescribed species

were deposited in the invertebrate collections of the California Academy of Sciences (San Francisco, California, USA). To ensure megafauna could be detected in the entire field of view, only the well-illuminated seafloor near the camera (the bottom half of each image) was annotated. The area coverage of this restricted field of view as determined by VARS (5.75 m^2) was used to calculate holothurian density. We calculated Spearman rank correlation coefficients (Siegel 1956) between weekly averages of salp percent cover and holothurian density, with the latter lagged at one-week intervals from 0 to -27 weeks. Resulting test statistics were compared to find the peak in correlation strength (highest Spearman ρ), and the range of lags for which correlations were significant ($p < 0.05$).

Salp carbon flux:

Decay adjustments-Salps partially decay as they sink from their living depths in surface waters through the water column to the deep sea. Because we measured carbon content of salps collected from shallow depths, we accounted for this decay using a temperature-dependent biomass decay ratio (Lebrato et al. 2011). We used a conservative depth of death of 100m based on salp depth distributions at Sta. M in June 2012 (Fig 1A), a sinking rate of 1009 m d^{-1} [average for *Salpa* in Lebrato et al. (2013)], a final depth of 4000m, and average Sta. M water temperatures recorded at 100m intervals through the water column from 2006-2012 (CTD records on ROV descents and ascents). We assumed that biomass decay rates were comparable to organic carbon decay rates. Based on this model, we estimated that carbon content of salps on the sea floor was 16% that of salps at a depth of 100 m (Fig.1B).

Tunic carbon flux- Organic carbon content of individual salps was estimated from representative *Salpa fusiformis* collected by ROV in March 2013 and adjusted for decay (Lebrato et al. 2011) as outlined above. Fourteen salps were placed individually in a petri dish with a

ruler, blotted dry and photographed from directly above using a Nikon D200 digital camera mounted on a tripod. Image J (Rasband 1997-2012) was used to calculate the area coverage for each salp in cm^2. Following this step each whole salp was freeze-dried, weighed, and analyzed for salt-corrected organic carbon content following the same methods used to estimate POC from sediment trap samples. Organic carbon content was then decay-adjusted by multiplying these values, derived in the laboratory from surface-collected specimens, by 0.16. The relationship between size and decayed carbon content of individual salps was found to be:

decayed organic carbon content of *Salpa fusiformis* = (salp area in $cm^2)^{0.9}$ x 0.15

as illustrated in Fig.1C. Using this relationship we calculated the decayed organic carbon content of an average sized salp (avg 5.2 cm^2 in our samples) to be 0.66 mg C per individual salp. This value was multiplied by the salp tunic flux (individual salps m^{-2} d^{-1}) measured from sediment trap collections to arrive at the salp tunic carbon flux (mg C m^{-2} d^{-1}).

Fecal pellet carbon flux- Salp fecal pellet carbon flux was calculated by multiplying the salp fecal pellet flux (number of salp fecal pellets m^{-2} d^{-1}) collected in the 600 mab sediment traps by 0.119 mg C per salp fecal pellet, an average value (Madin 1982; Wilson et al. 2013).

Salp detrital aggregate flux- Salp aggregate organic carbon flux was estimated following a method previously used to determine phytodetrital aggregate organic carbon flux (Smith et al. 1998; Smith et al. 1994). The supply of carbon to sediment communities through the decay of salp aggregates on the seafloor, or salp detrital aggregate flux, was calculated by dividing decayed organic carbon per area coverage of salps by residence times of 109 h and 365 h, the duration for which two individual salps were visible on the sea floor in hourly time lapse camera images taken at Sta. M in April and May 2012, using the formulae:

Salp detrital aggregate organic carbon $flux_{109}$ = 0.15 x (salp detrital aggregate percent cover x 100)$^{0.9}$ x (24/109)

Salp detrital aggregate organic carbon $flux_{365}$ = 0.15 x (salp detrital aggregate percent cover x 100)$^{0.9}$ x (24/365)

Net carbon- Carbon flux curves were integrated over a period from November 2011 to November 2012 using the trapezoidal rule (Hall, 1876) to calculate the area under the curves and estimate total organic carbon supply or total organic carbon demand (mg C m^{-2}) for the entire period.

Analytical approach:

The study of the salp bloom and its impact on abyssal processes is presented here first from a long-term perspective of the 24-year time series at Sta. M, 1989 through 2012, and then more closely examined over a one-year segment between November 2011 and November 2012. This study was further narrowed to the salp bloom and deposition event that spanned a nearly 6-month period from 1 March through 23 August 2012. We trace the evolution of this episodic carbon transport and mineralization event in time-series from primary production, the abundance and composition of salps and other zooplankton in surface waters, salp distribution in the water column, the flux of salp detritus from sediment traps to the sea floor and the mineralization rates using carbon as the common denominator. In addition, we monitored the change in abundance of a dominant megafaunal species over a one year period encompassing the salp deposition event.

Results

24-year time-series: Surface Chl-*a* concentration, derived from satellite color over a 100-km radius circle above Sta. M, beginning in 1996, exhibited seasonal highs in spring and summer with a tendency toward increasing duration of peaks especially notable since 2010 (Fig. 2A).

Similarly, satellite-inferred NPP was elevated each spring and summer with higher peaks over the last seven years (Fig. 2B). Displacement volume of large and small zooplankton in the upper 210 m of the water column, collected seasonally in the vicinity of Sta. M, showed a marked increase in displacement volume during 2011-2012 compared to the previous twenty years (Fig. 2C). However, peaks of equivalent magnitude were recorded each decade from 1951-1989 (Lavaniegos and Ohman 2007; CalCOFI website http://www.data.calcofi.org/zooplankton/calcofi-nets-description.html). The carbon biomass of salps from springtime samples collected inshore of CalCOFI station 70 (Lavaniegos and Ohman 2007) was above the long-term mean for the period 1989-2012 (blue symbol, Fig. 2D; note log scale), but in the offshore region (stations 80-120, lines 80-93) was the highest value in the 24-year time series (red symbol, Fig. 2D; note log scale). At least 13 species of salps were identified from the spring 2012 samples, but 99% of the salp carbon biomass was *Salpa aspera*. As with displacement volume, comparable salp carbon biomass values have been observed in decades preceding 1989 (Lavaniegos and Ohman 2007).

The sinking flux of particulate organic carbon (POC) at 3400 m depth (600 mab) exhibited two major peaks in POC flux over the last 18 months of the time series, the highest on record at Sta. M. One peak occurred in June 2011, and another between March and May 2012 corresponding to peaks in surface ocean Chl-*a* and primary production (Fig. 2E). The peak POC flux in June 2011 was the highest recorded over the 24-year time series, with the predominant constituent being the diatom *Rhizosolenia* (*R. setigera and R. styliformis*), which can form large blooms in surface waters before sinking into the deep sea. The major peak in POC flux in March 2012 (Fig. 2E) included a relatively high number of salps, as tunics and fecal pellets, originating from the upper 500 m of the water column (Fig. 1A). This spring 2012 peak in POC flux was

followed by another major sedimentation event in September, which consisted of a combination of salp fecal pellets and phytodetritus (Fig. 2E).

On the seafloor, daily phytodetrital aggregate cover (Fig. 2F; black line) was higher in 2012 than any previous year. The salp deposition event from March through late August 2012 was the largest detrital aggregate deposition event on record, with daily seafloor coverage 6.7 times higher than any pre-2012 peak (Fig. 2F, red line). This salp deposition event was followed by a peak in phytodetrital aggregate cover in late August and September, which reached four times the coverage of any pre-2012 peak. The response of the sediment community, estimated by sediment community oxygen consumption (SCOC), also showed record peaks concurrent with these deposition events (Fig. 2G). It is interesting that a smaller peak in SCOC during 1991 coincided with a peak in salp carbon biomass (Fig. 2D).

November 2011 to November 2012:

Surface Chl-*a* reached a high of 0.9 mg m^{-3} in late June and early July 2012, concurrent with a peak in the estimated net primary production of 988 mg C $m^{-2}d^{-1}$ (Fig. 3A). Compared to the average values for the entire dataset (1951-2013) displacement volume of zooplankton was anomalously high during the April 2012 net-tow sampling (large zooplankton: 237 ml m^{-2} anomaly; small zooplankton 40 ml m^{-2} anomaly; Fig. 3B). During the following sampling in July 2012, both size fractions of zooplankton returned to the long-term mean displacement volume values.

Living salps, tentatively identified as *Salpa spp.*, were most abundant in the upper 500 m of the water column as observed during two ROV dives in June 2012 (Fig. 1A). Over 99% of midwater sightings occurred shallower than 600m depth, as estimated from vertical transects through the water column. Salp tunics were otherwise rare in the water column. As noted above,

zooplankton net tows conducted by the CalCOFI program during April 2012 in the vicinity of Sta. M were dominated by *Salpa aspera*. Given these data, we are referring to the salps on the sea floor at Sta. M. as *Salpa spp*. because no seafloor specimens were collected during this period.

The POC flux increased sharply beginning in early March 2012 with a peak of 38 mg C $m^{-2}d^{-1}$ in mid-April before declining precipitously over the next two months (Fig. 3C). The decline in this measure might be due to the clogging of the sediment traps between mid-May and early June until the mooring was recovered and then redeployed in mid-June. The POC flux rose with a secondary peak in September before the traps appeared to have clogged once again. These periods of high flux in spring and early fall were well above the mean POC flux over the entire 24-year period (7 ± 6 mg C m^{-2} d^{-1}), reaching positive anomalies of 30 mg C m^{-2} d^{-1} in April (Fig. 3C).

Salp fecal pellets in the sediment trap collections were distinguishable in small numbers beginning in mid-November 2011 but became more prevalent the following year from early March through the end of June, peaking between 20 to 30 March and 14 to 24 June at 40 salp fecal pellets m^{-2} d^{-1} at 600 mab (Fig. 3D). Until these spring peaks, the quantity of salp fecal pellets did not exceed 10 fecal pellets $m^{-2}d^{-1}$ during the time series from 1993 through 2012. The estimated carbon content of the fecal pellets reached 4.7 mg C $m^{-2}d^{-1}$ in late March and mid-June (Fig. 3D). Salp tunics were collected in sediment traps between 19 April and 18 May 2012, but in numbers ≤ 8 per ten-day sampling period perhaps because of the difficulty of such large particles passing through the sediment trap baffle.

In April and May 2012, a peak in POC flux coincided with peaks in the percent of the sea floor covered with salp detritus (Fig. 3E). The coverage rose sharply in the beginning of April,

reaching a high of 58% cover throughout most of the month then declining in May. The second increase in salp detrital coverage began in late May and reached a high of 98% from late June and early July before declining below 1% by the second week in August (Fig. 3E). This second peak corresponded with a negative anomaly in POC flux. The surface sediment fluorescence increased slightly at the beginning of each salp detrital peak, but then declined while the salps covered a substantial portion of the sea floor (Fig. 3E). The highest fluorescence in the seafloor surface sediments occurred in September, coinciding with a large phytodetrital deposition event.

The sediment community responded to these pulses of detritus with sustained anomalously high SCOC starting with the initial stages of the first salp deposition and extending over a month past the phytodetrital deposition event. SCOC reached a peak of 31 mg C $m^{-2}d^{-1}$ corresponding to maximum salp coverage on the sea floor (Fig. 3F). The peaks in SCOC during June represent the highest recorded rates measured at Sta. M over the 24 year time series. There was no perceptible lag between the arrival of salp detritus and phytodetritus on the seafloor and the increased SCOC. The high fluorescence in the seafloor surface sediment during the early stages of the salp deposition peaks suggests that material with a high content of chlorophyll reached the seafloor in a relatively non-degraded state (Fig. 3E).

A numerically dominant species of mobile megafauna, the holothuroid *Peniagone* sp. nov. (voucher CASIZ XXXXXX), ranged from a weekly average of 0.3 individuals m^{-2} from November 2011 until early July 2012, when the density sharply increased and attained a peak of 1.1 individuals m^{-2} in late September and early October (Fig. 3G). This increased density of *Peniagone* sp. nov. continued through the summer and early fall reaching the highest peak of 1.2 individuals m^{-2} in weekly averages, at the end of September before declining (Fig. 3G). Density of *Peniagone* sp. nov. was significantly correlated with salp detrital aggregate percent cover

362 ($p<0.05$) when lagged by 7 to 25 weeks. The strength of this correlation peaked with a lag of 14
363 weeks (Spearman $\rho = 0.7866$, $p < 0.0001$). *Peniagone* densities estimated from Benthic Rover
364 transit images over the same time period ranged from 0.5-1.3 individuals m^2. These animals were
365 often observed over patches of salp detritus and phytodetritus, in a suggested feeding posture
366 with oral tentacles engaged with the detrital material.

367 **March through 23 August 2012**:

368 The POC flux over this six-month period was highest in mid-April with declining fluxes
369 from late May through June (Fig. 4A). This decline was probably the result of sediment trap
370 clogging events, especially given the large number of salp tunics reaching the sea floor over that
371 time period. The peaks in salp fecal pellet carbon flux reached 5 mg C $m^{-2}d^{-1}$ at 600 mab and
372 accounted for 10% of the total carbon deposited over this period (220 mg C m^{-2} as salp fecal
373 pellet carbon, of 2279 mg C m^{-2} total POC collected in sediment traps; Fig. 4A). Salp tunic
374 organic carbon flux at 600 mab did not exceed 0.5 mg C m^{-2} d^{-1}.

375 The salp detrital aggregate carbon flux on the sea floor ranged from 0 to 130 mg C $m^{-2}d^{-1}$
376 over this six-month period (Fig. 4B). The estimated supply of organic carbon from salp detritus
377 over this time period, based on integration of the flux curve, was 2713 mg C m^{-2} for salps
378 decaying over a conservative 365-hour residence time. This salp supply represents a 19%
379 increase over the POC supply estimated from trap samples over the same period of time. Using a
380 residence time of 109 h for salp detritus, the organic carbon supply was estimated to be 9086 mg
381 C m^{-2} (Fig. 4B). Based on these estimates, food supply from salp detritus provided from 97%
382 (365 h residence time) to 327% (109 h residence time) of the demand estimated from SCOC over
383 the six-month period. This salp deposition event clearly provided a major influx of organic
384 carbon to the sea floor.

SCOC began to increase slowly beginning in early March reaching a series of peaks extending from early June through the later part of July before slowly declining (Fig. 4C). The highest SCOC was 31 mg C $m^{-2}d^{-1}$ in mid-June. Increased SCOC corresponded with the peaks in salp detritus percent cover and estimated POC flux on the sea floor (Fig. 4B). There was an immediate response in SCOC to the salp fluxes as detected with daily resolution. No temporal lag existed in cross correlations between salp detrital aggregate C flux and Benthic Rover SCOC (time lag = 0, r_s =0.69, $p < 0.001$). After the highs in SCOC during June and July, the rates declined only to increase again in late August. The summed demand for organic carbon, SCOC, over the period from 1 March to 23 August was 2781 mg C m^{-2} (Fig. 4C).

The balance of food supply to and demand by the sediment community over the six month period was estimated by calculating the difference between total food supply (the greater of POC flux or salp detritus flux on the sea floor for any given period), and food demand (SCOC for that same period), and integrating the plot of this value over time. This estimate of supply conservatively accounts for any overlap in salp organic carbon flux and POC flux sources. Although some portion of the POC flux was invariably included in the salp pulse, most of the POC flux consisted of smaller particulate matter that excluded a large fraction including the majority of salp tunics because of the small size of the sediment trap baffle openings (hexagonal grid, 1.5 cm/side). Because both carbon supply estimates overlap and are not mutually exclusive, we chose to use the salp detritus estimates for the range of food reaching the sea floor. The net organic carbon supply exceeded the SCOC demand consistently from March until the end of June using both the 365 and 109 hour residence time estimates for salp tunics (Fig. 4D). A deficit in food supply followed through July and August.

Discussion

408 The salp bloom in spring 2012 at Sta. M provided an exceptionally high supply of
409 organic carbon to the benthic community, which rapidly utilized this rich planktonic food source
410 over a period of at least several months. Although not observed frequently at Sta. M, such
411 blooms provide an excellent conduit for the rapid transfer of primary producers to the abyssal sea
412 floor.

413 Pelagic tunicates, specifically salps, provide an efficient mechanism to consume primary
414 production in surface waters and export it to the deep ocean. Salps are adept at filtering small
415 particulate matter $\geq$ 0.7 µm from the water column (Harbison et al. 1986), ultimately forming
416 compact fecal pellets that sink rapidly to the deep ocean (Andersen 1998). Salp blooms occur
417 primarily in the upper 100 m of the water column with densities up to 1000 individuals m^{-3}
418 (Andersen 1998). However, swarms of *Salpa aspera* can undergo diel vertical migrations to
419 depths of 600 to 800 m as observed in the western north Atlantic (Madin et al. 2006; Wiebe et al.
420 1979). The continuous feeding behavior of salps (Madin 1974) can result in a substantial
421 reduction in surface phytoplankton in one day during such blooms (Bathmann 1988; Perissinotto
422 and Pakhomov 1998). The coincidence of the high concentration of salps and low chlorophyll in
423 April 2012 at Sta. M (Fig. 2A,B) might be attributable to extensive grazing pressure on
424 phytoplankton by salps.

425 Most species of salps, including *Salpa* spp, have high defecation rates (Madin 1982) and
426 form large compact fecal pellets that sink rapidly at velocities up to 2700 m d^{-1}(Bruland and
427 Silver 1981). Salp fecal pellets vertically transport organic matter to the deep ocean with C:N
428 ratios of 5.4 to 6.2, which are similar to those of living plankton (Bruland and Silver 1981).
429 Cyanobacteria incorporated in salp fecal material represent a small size fraction of the particulate
430 matter originating in surface waters and traced to the abyssal sea floor in the eastern north

Atlantic (Pfannkuche and Lochte 1993). During the vertical flux of *Salpa* spp. fecal pellets through the water column, a 36% loss in carbon content was found between 200 and 900 m depth in the central north Pacific (Iseki 1981). Similar losses were found in organic carbon, nitrogen and lipid content of salp fecal material between 740 and 4240 m in the eastern North Pacific (Matsueda et al. 1986). At Sta. M, salp fecal pellets were estimated to have contributed 10% of the total POC flux (220 of 2279 mg C m^{-2}) over the duration of the salp pulse (Fig 4A).

Of studies published to our knowledge, estimates of organic carbon flux associated with salp fecal pellets from surface waters to depths up to 4240 m spanned four orders of magnitude (Table 1). The lowest flux, 0.01 mg C $m^{-2}d^{-1}$, was recorded for *Salpa cylindrica* in the northwestern Atlantic (Caron et al. 1989) and the highest flux, 142 mg C $m^{-2}d^{-1}$, was measured for *Cyclosalpa pinnata* in the central North Atlantic (Madin 1982). The salp fecal pellet carbon flux measured at Sta. M falls within this large range and closely agrees with similar measurements from sediment trap collections at similar depths in the northeastern Pacific (Matsueda et al. 1986; Table 1).

On the sea floor, salp tunics have been observed previously to depths of 3000 m in the western North Atlantic. Wiebe and associates (1979) estimated from trawl results that 0.4% of a migrating swarm of *Salpa aspera* died per day and their sinking flux contributed 3.6 mg C $m^{-2}d^{-1}$ to the benthic food supply (Table 1). They estimated that the combined daily contribution of fecal pellets and tunics would supply 180% of the daily metabolic demand of the sediment community at slope depths (Wiebe et al. 1979). Using our conservative estimate of a 365 h residence time, salp detrital aggregates alone would have contributed 2713 mg C m^{-2} during the period of the salp pulse (Fig 4B), almost enough to fuel the demand of the sediment community (2781 mg C m^{-2}; Fig 4 C). Again using this conservative estimate, net organic carbon flux was

positive almost continuously from the beginning of the pulse in early March through mid-June, when SCOC exceeded instantaneous supply.

Salp fecal pellets also comprise a useful food source to benthic communities at abyssal depths. They have been collected in sediment cores from 4500 to 4800 m in the eastern North Atlantic (Pfannkuche and Lochte 1993), and this salp fecal material containing cyanobacteria was identified in the guts of two species of benthic holothuroids and their fecal casts (Pfannkuche and Lochte 1993). In the southwestern Pacific, benthic crustaceans were observed feeding on tunics of the salp, *Thetys vagina*, at depths between 200 and 2500 m depth (Henschke et al. 2013).

We observed an increase in abundance of *Peniagone* sp. nov. by a factor of seven approximately 14 weeks after the salp deposition began on the seafloor at Sta. M (Fig. 3G). These animals were often observed in a feeding posture over salp tunics. The surface water salp bloom in spring 2012 was wide-spread covering extensive areas along the central and southern California coast, including waters over Sta. M and out to at least 650 km offshore (M. Ohman and L. Sala, pers. comm.). The large increase in the population of *Peniagone* sp. nov. lagged 14 weeks behind the salp deposition, which suggests a major immigration response rather than reproduction alone. Although we do not know the growth rate of *Peniagone* sp. nov., to our knowledge the maximum growth rate estimated for a congener is 6mm $month^{-1}$ (Ruhl 2007). This growth rate would be insufficient to allow new recruits to reach the minimum size of individuals observed during the *Peniagone* sp. nov. population peak (minimum length 4.1 cm; L. Clary pers. comm.). The question arises as to where these immigrant animals came from given the wide-spread coverage of the salp bloom in overlying waters and assuming similar deposition conditions over a large area of the sea floor. Members of the genus *Peniagone* are capable of

swimming (Miller and Pawson 1990; Rogacheva et al. 2012). We have frequently observed *Peniagone* sp. nov. swimming in video images by flexing their entire body in longitudinal muscle expansions and contractions in the water above the sediment. This mobility greatly increases this animal's ability to cover larger areas of the seafloor compared to most other members of the megafauna at Sta. M that are restricted to the seafloor. These observations are very intriguing but must await further examination of the size distribution of *Peniagone* at Sta. M and the estimated spatial and temporal extent of the salp bloom in surface waters.

Other gelatinous zooplankton form blooms in surface waters and export large amounts of organic carbon to the deep-sea floor. In the Arabian Sea, there was a large deposition of jellyfish, *Crambionella orsini*, recorded on the seafloor between 300 and 3300 m depth (Billett et al. 2006). The contribution of this deposition event was estimated to be as high as 78 g C m^{-2}, which would exceed the annual particulate organic carbon flux estimated from sediment trap collections in this region. A similar deposition event of carcasses of the pyrosome, *Pyrosoma atlanticum*, occurred in the eastern equatorial Atlantic, with estimated organic contributions up to 22 g C m^{-2} at depths to 1275 m (Lebrato and Jones 2009).

More generally, zooplankton appear to have an important but ill-defined role in facilitating carbon transport and sequestration in the ocean. Both passive and active transport by mesozooplankton are significant processes in the southern California Current System (Stukel et al. 2013). Global-scale biogeochemical models are driven mainly by the supply of nutrients, which in some cases can then drive fast and slow sinking flux of POC (e.g. Yool et al. 2013). However, such models do not include mechanisms to represent the episodic carbon fluxes observed here (e.g. Lampitt et al. 2009). Such episodic fluxes are also likely to have substantially different POC attenuation curves with depth compared to the 'steady state' conditions

represented in static attenuation curves (e.g. Martin et al. 1987; Buesseler et al. 2007). It remains unclear as to how global scale models might reproduce these major episodic events while still having a reasonable number of state and rate variables and parameters (i.e. reasonable complexity).

Large episodic pulses of particulate organic carbon reach the abyssal sea floor and serve as a vital food supply to sustain the benthic community at Sta. M. The increased frequency of these food pulses over the last several years, especially the 2012 salp deposition event, was unprecedented over the 24-years of monitoring this station.

REFERENCES:

Andersen, V. 1998. Salp and pyrosomid blooms and their importance in biogeochemical cycles, p. pp. 125-137. *In* Q. Bone [ed.], The biology of pelagic Tunicates. Oxford University Press.

Baldwin, R., R. Glatts, and K. Smith Jr. 1998. Particulate matter fluxes into the benthic boundary layer at a long time-series station in the abyssal NE Pacific: composition and fluxes. Deep Sea Research Part II: Topical Studies in Oceanography **45:** 643-665.

Bathmann, U. 1988. Mass occurrence of *Salpa fusiformis* in the spring of 1984 off Ireland: implications for sedimentation processes. Marine Biology **97:** 127-135.

Behrenfeld, M. J., and P. G. Falkowski. 1997. Photosynthetic rates derived from satellite-based chlorophyll concentration. Limnology and Oceanography **42:** 1-20.

Berner, L. D. 1967. Distribution atlas of *Thaliacea* in the California Current region, p. 1-322. California Cooperative Oceanic Fisheries Investigations Atlas.

Billett, D., B. Bett, C. Jacobs, I. Rouse, and B. Wigham. 2006. Mass deposition of jellyfish in the deep Arabian Sea. Limnology and Oceanography **51:** 2077-2083.

Bruland, K. W., and M. W. Silver. 1981. Sinking rates of fecal pellets from gelatinous zooplankton (salps, pteropods, doliolids). Marine Biology **63:** 295-300.

Buesseler, K. O. and others 2007. Revisiting carbon flux through the ocean's twilight zone. Science **316:** 567-570.

Harbison, G. R., V. L. Mcalister, and R. W. Gilmer. 1986. The response of the salp, *Pegea confoederata*, to high levels of particulate material: starvation in the midst of plenty. Limnology and Oceanography **31:** 371-382.

Henschke, N. and others 2013. Salp-falls in the Tasman Sea: a major food input to deep-sea benthos. Marine Ecology Progress Series **491:** 165-175.

Henthorn, R. G., B. W. Hobson, P. R. McGill, A. Sherman, and K. L. Smith. 2010. MARS Benthic Rover: in-situ rapid proto-testing on the Monterey Accelerated Research System. IEEE Xplore**:** 1-7.

Iseki, K. 1981. Particulate organic matter transport to the deep sea by salp fecal pellets. Marine Ecology Progress Series **5:** 55-60.

Kahru, M., R. Kudela, M. Manzano-Sarabia, and B. G. Mitchell. 2009. Trends in primary production in the California Current detected with satellite data. Journal of Geophysical Research: Oceans (1978-2012) **114**. doi 10.1029/2008JC004979

Kahru, M., R. M. Kudela, M. Manzano-Sarabia, and B. Greg Mitchell. 2012. Trends in the surface chlorophyll of the California Current: Merging data from multiple ocean color satellites. Deep Sea Research Part II: Topical Studies in Oceanography **77:** 89-98.

Lampitt, R. S., I. Salter, and D. Johns. 2009. Radiolaria: major exporters of organic carbon to the deep ocean. Global Biogeochemical Cycles **23: GB1010**.

Lavaniegos, B. E., and M. D. Ohman. 2003. Long-term changes in pelagic tunicates of the California Current. Deep Sea Research Part II: Topical Studies in Oceanography **50:** 2473-2498.

---. 2007. Coherence of long-term variations of zooplankton in two sectors of the California Current System. Progress in Oceanography **75:** 42-69.

Lebrato, M. and others 2013. Jelly biomass sinking speed reveals a fast carbon export mechanism. Limnology and Oceanography **58:** 1113-1122.

555 Lebrato, M., and D. Jones. 2009. Mass deposition event of *Pyrosoma atlanticum* carcasses off
556 Ivory Coast (West Africa). Limnology and Oceanography **45:** 1197-1209.
557 Lebrato, M. and others 2011. Depth attenuation of organic matter export associated with jelly
558 falls. Limnology and Oceanography **56:** 1917-1928.
559 Madin, L., P. Kremer, P. Wiebe, J. Purcell, E. Horgan, and D. Nemazie. 2006. Periodic swarms
560 of the salp *Salpa aspera* in the slope water off the NE United States: biovolume, vertical
561 migration, grazing, and vertical flux. Deep Sea Research Part I: Oceanographic Research
562 Papers **53:** 804-819.
563 Madin, L. P. 1974. Field observations on the feeding behavior of salps (Tunicata: Thaliacea).
564 Marine Biology **25:** 143-147.
565 ---. 1982. Production, composition and sedimentation of salp fecal pellets in oceanic waters.
566 Marine Biology **67:** 39-45.
567 Martin, J. H., G. A. Knauer, D. M. Karl, and W. W. Broenkow. 1987. VERTEX: Carbon cycling
568 in the northeast Pacific. Deep Sea Research Part A. Oceanographic Research Papers **34:**
569 267-285.
570 Matsueda, H., N. Handa, I. Inoue, and H. Takano. 1986. Ecological significance of salp fecal
571 pellets collected by sediment traps in the eastern North Pacific. Marine Biology **91:** 421-
572 431.
573 McGill, P. R., A. D. Sherman, B. W. Hobson, R. G. Henthorn, and K. L. Smith Jr. 2009. Initial
574 deployments of the Rover, an autonomous bottom-transecting instrument platform. The
575 Journal of Ocean Technology **4:** 54-70.

576 Miller, J. E., and D. L. Pawson. 1990. Swimming sea cucumbers (Echinodermata:
577 Holothuroidea): a survey with analysis of swimming behavior in four bathyal species.
578 Smithsonian Contributions to Marine Science **35:** 1-18.
579 Morris, R., Q. Bone, R. Head, J. Braconnot, and P. Nival. 1988. Role of salps in the flux of
580 organic matter to the bottom of the Ligurian Sea. Marine Biology **97:** 237-241.
581 Ohman, M. D., and P. Smith. 1995. A comparison of zooplankton sampling methods in the
582 CalCOFI time series. California Cooperative Oceanic Fisheries Investigations Report**:**
583 153-158.
584 Perissinotto, R., and E. Pakhomov. 1998. Contribution of salps to carbon flux of marginal ice
585 zone of the Lazarev Sea, Southern Ocean. Marine Biology **131:** 25-32.
586 Pfannkuche, O., and K. Lochte. 1993. Open ocean pelago-benthic coupling: cyanobacteria as
587 tracers of sedimenting salp faeces. Deep Sea Research Part I: Oceanographic Research
588 Papers **40:** 727-737.
589 Rasband, W. S. 1997-2012. ImageJ. National Institutes of Health.
590 Rogacheva, A., A. Gebruk, C. H. Alt, A. Kroh, and M. Reich. 2012. Swimming deep-sea
591 holothurians (Echinodermata: Holothuroidea) on the northern Mid-Atlantic Ridge.
592 Ruhl, H. A. 2007. Abundance and size distribution dynamics of abyssal epibenthic megafauna in
593 the northeast Pacific. Ecology **88:** 1250-1262.
594 Schlining, B. M., and H. J. Stout. 2006. MBARI's Video Annotation and Reference System.
595 IEEE Xplore.
596 Sherman, A. D., and K. L. Smith. 2009. Deep-sea benthic boundary layer communities and food
597 supply: A long-term monitoring strategy. Deep Sea Research Part II: Topical Studies in
598 Oceanography **56:** 1754-1762.

599 Siegel, S. 1956. Nonparametric stats for the behavioral sciences. McGraw-Hill Book Company.
600 Silver, M. W., and K. W. Bruland. 1981. Differential feeding and fecal pellet composition of
601 salps and pteropods, and the possible large-scale particulate organic matter transport to
602 the deep sea. Marine Biology **53:** 249-255.
603 Smith Jr., K. L. 1987. Food energy supply and demand: A discrepancy between particulate
604 organic carbon flux and sediment community oxygen consumption in the deep ocean.
605 Limnology and Oceanography **32:** 201-220.
606 Smith Jr., K. L., R. J. Baldwin, R. C. Glatts, R. S. Kaufmann, and E. C. Fisher. 1998. Detrital
607 aggregates on the sea floor: Chemical composition and aerobic decomposition rates at a
608 time-series station in the abyssal NE Pacific. Deep Sea Research Part II: Topical Studies
609 in Oceanography **45:** 843-880.
610 Smith Jr., K. L., R. J. Baldwin, H. A. Ruhl, M. Kahru, B. G. Mitchell, and R. S. Kaufmann.
611 2006. Climate effect on food supply to depths greater than 4,000 meters in the northeast
612 Pacific. Limnology and Oceanography **51:** 166-176.
613 Smith Jr., K. L., and E. R. M. Druffel. 1998. Long time-series monitoring of an abyssal site in
614 the NE Pacific: an introduction. Deep Sea Research II **45:** 573-586.
615 Smith Jr., K. L. and others 1997. An autonomous, bottom-transecting vehicle for making long
616 time-series measurements of sediment community oxygen consumption to abyssal
617 depths. Limnol. Oceanogr **42:** 1601-1612.
618 Smith Jr., K. L., and R. S. Kaufmann. 1999. Long-term discrepancy between food supply and
619 demand in the deep eastern North Pacific. Science **284:** 1174-1177.

620 Smith Jr., K. L., R. S. Kaufmann, and R. J. Baldwin. 1994. Coupling of near-bottom pelagic and
621 benthic processes at abyssal depths in the eastern North Pacific Ocean. Limnology and
622 Oceanography **39:** 1101-1118.
623 Smith Jr., K. L., R. S. Kaufmann, and W. W. Wakefield. 1993. Mobile megafaunal activity
624 monitored with a time-lapse camera in the abyssal North Pacific. Deep Sea Research Part
625 I: Oceanographic Research Papers **40:** 2307-2324.
626 Smith Jr., K. L., H. Ruhl, M. Kahru, C. L. Huffard, and A. Sherman. in press. Deep ocean
627 communities impacted by changing climate over 24 in the abyssal northeast Pacific
628 Ocean. Proceedings of the National Academy of Sciences.
629 Smith Jr., K. L., H. A. Ruhl, B. J. Bett, D. S. M. Billett, R. S. Lampitt, and R. S. Kaufmann.
630 2009. Climate, carbon cycling, and deep-ocean ecosystems. Proceedings of the National
631 Academy of Sciences **106:** 19211-19218.
632 Smith Jr., K. L., H. A. Ruhl, R. S. Kaufmann, and M. Kahru. 2008. Tracing abyssal food supply
633 back to upper-ocean processes over a 17-year time series in the northeast Pacific.
634 Limnology and Oceanography **53:** 2655.
635 Strickland, J. D. H., and T. R. Parsons. 1972. A practical handbook of seawater analysis.
636 Fisheries Research Board of Canada.
637 Thomas, L. and others 2010. Distance software: design and analysis of distance sampling
638 surveys for estimating population size. Journal of Applied Ecology **47:** 1365-2664.
639 Wakefield, W. W., and A. Genin. 1987. The use of a Canadian (perspective) grid in deep-sea
640 photography. Deep Sea Research Part A. Oceanographic Research Papers **34:** 469-478.

641 Wiebe, P. H., L. P. Madin, L. R. Haury, G. R. Harbison, and L. M. Philbin. 1979. Diel vertical
642 migration by *Salpa aspera* and its potential for large-scale particulate organic matter
643 transport to the deep-sea. Marine Biology **53:** 249-255.
644 Wilson, S. E., H. A. Ruhl, and K. L. Smith. 2013. Zooplankton fecal pellet flux in the abyssal
645 northeast Pacific: A 15 year time-series study. Limnolology Oceanography **58:** 881-892.
646 Yool, A., E. Popova, and T. Anderson. 2013. MEDUSA-2.0: an intermediate complexity
647 biogeochemical model of the marine carbon cycle for climate change and ocean
648 acidification studies. Geoscientific Model Development Discussions **6:** 1259-1365.

649

650

Table

Table 1. Comparison of salp fecal pellet and tunic carbon fluxes estimated in nine other studies conducted in seven different regions of the world ocean.*Only salp standing stock presented (mg C m^{-2}).

Region	Sample depth (m)/water depth if available	Collection method	Direct measures	Total POC flux	Salp carbon flux (mg C m^{-2} d^{-1})		Taxon	Citation
					fecal pellets	tunics		
W. N. Atlantic	/~2000	Trawls	Salp biomass, defecation rates in aquaria		8.5-137	3.6	*S. aspera*	Wiebe et al. 1979
	25/	SCUBA and trawl			0.01-0.04		*S. cylindrica*	
	50/	SCUBA and trawl			0.01-0.07		*S. cylindrica, S. maxima, Pegea confoederata*	
Central N. Atlantic	25m/ 3300	SCUBA	Defecation rates in aquaria, fecal pellet organic carbon content		142 ± 72		*Cyclosalpa pinnata*	Madin 1982
	100/				0.04-0.3			
	to 500/				0.8-23.4			
Southern Ocean	0-1000m/	Trawl	Salp ingestion rates, biomass		88		*S. thompsoni*	Perissinotto and Pakhomov 1988
	140/			8.8				
	300/			2.6				
S.W. Pacific	237-1831/	Trawl	Total biomass, gut-free salp tunic organic carbon content			*3.1-26.1	*Thetys vagina*	Henschke et al. 2013
	200/			10.5				
	900/			6.7				
	740/				23			
	940/				18			
	1440/				6.7			
	3440/				6.7			
	4240/				8.7			
N.E. Pacific	3400/4000	Sediment traps, ROV collection	Fecal pellet flux, salp whole tunic flux, total POC flux, salp organic carbon content	≤53	<4.8	≤0.5	*S. fusiformis*	This paper

Figure legends:

Figure 1. Data used to estimate salp carbon. (A) Vertical distribution and abundance of salps at Sta. M in June 2012 as determined from vertical transects through the water column at 35 m min^{-1}. Note log scale of X axis. (B) Salp biomass export ratio (M x $M0^{-1}$ = biomass at depth x biomass at $surface^{-1}$) used to estimate decayed carbon content of salps on the seafloor. Equations in Lebrato et al. (2013) were applied to a sinking speed of 1009 m d^{-1}, depth of death of 100m, and temperatures recorded at Sta. M since 2006. (C) Relationship between salp tunic area coverage and estimated decayed organic carbon content.

Figure 2. Long time-series measurements of surface ocean to benthic parameters from July 1989 through November 2012 at Sta. M in the northeast Pacific Ocean. Dashed lines on axes indicate data gaps exceeding one month (A) Chl- *a* concentration around Sta. M (100 km radius circle). (B) Net primary production (NPP) around Sta. M. (100 km radius circle). (C) Displacement volume of large (> five mL, open circles) and small (< five mL, black circles) zooplankton. (D) Salp biomass carbon content. Carbon biomass of salps in the more inshore region (black and open symbols) and the offshore (red symbol). (E) POC flux measured from sediment traps, with ten day resolution. (F) Percent seafloor coverage of salp (red line) and phytoplankton-derived (black line) detrital aggregates, daily average from camera tripod images. (G) SCOC measured seasonally from 1989 until 2011 and monthly averages of daily measurements taken from 2011 through 2012. Oxygen consumption has been converted to mg carbon using a respiratory quotient of 0.85 (Smith 1987). Panels A, B, E, F and G are adapted from Smith et al. (in press).

Figure 3. Surface water conditions, POC flux and benthic community responses over a time series from 1 November 2011 to 30 November 2012 at Sta. M. (A) Chl-*a* concentration (black

679 line) and net primary production (red line, right y-axis). (B) Zooplankton displacement volume
680 anomaly from full time series mean (1951-2013), small zooplankton (black circles, difference
681 from overall mean of 32 ml m^{-2}), large zooplankton (open circles, difference from overall mean
682 of 9 ml m^{-2}). (C) POC flux (black line) and anomaly from full time-series mean of 7.3 mg C m^{-2}
683 d^{-1}. Positive anomalies are shown in blue, negative anomalies are shown in red. (D) Salp fecal
684 pellet flux (red line, right y-axis) measured from sediment traps and estimated salp fecal pellet
685 carbon flux (black line) estimated using an average of 0.119 mg C $pellet^{-1}$. (E) Percent cover
686 over the sea floor of phytodetrital aggregates (black line) and salp detrital aggregates (dashed
687 line). Mean fluorescence value measured by Rover showing relative seafloor excitation at 675
688 nm (red line, right y-axis). (F) SCOC (black line) and anomaly (positive in blue, negative in red)
689 from overall time-series mean of 11.26 mg C m^{-2} d^{-1}. (G) Weekly averages of daily images of
690 *Peniagone* sp nov. density taken by the time-lapse camera tripod, 95% confidence limits (gray
691 line) around the equation $f = y_0 + a \times e^{(-0.5(\ln(x/0)/b)\^2)}$ with R^2 value 0.58.
692 **Figure 4**. Carbon supply and demand during salp pulse, from 1 March-23 Aug 2012. (A) POC
693 flux (black line, integrated curve = 2279 mg C m^{-2}) and salp fecal pellet organic carbon flux (red
694 line. integrated curve = 220 mg C m^{-2}). (B) Salp detrital aggregate organic carbon flux minimum
695 estimates based on a residence time of 365 h (red line, integrated curve = 2713 mg C m^{-2}) and
696 maximum estimates based on a residence time of 109 h (black line, integrated curve = 9086 mg
697 C m^{-2}). (C) SCOC, integrated curve = 2781 mg C m^{-2}). (D) Estimated net organic carbon supply
698 (the higher of POC flux or salp organic carbon flux) – SCOC, based on residence times of 365 h
699 (red line, integrated curve = 349 mg C m^{-2}) and 109 h (black line, integrated curve = 4447 mg C
700 m^{-2}).
701

Figure 1.

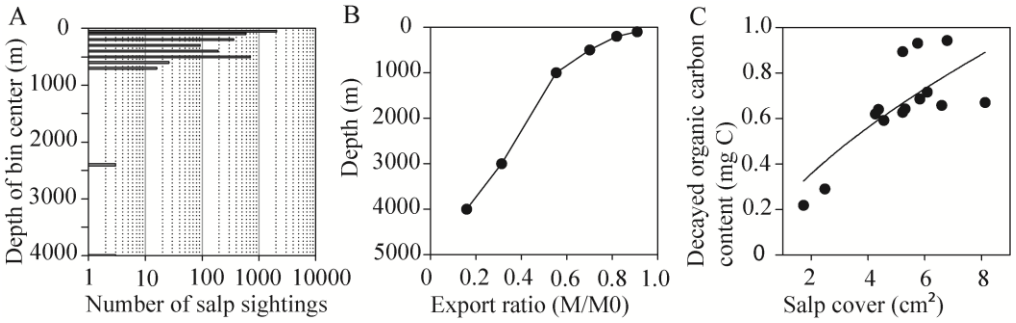
A
Depth of bin center (m)
0
1000
2000
3000
4000
1
10
100
1000
10000
Number of salp sightings
B
Depth (m)
0
1000
2000
3000
4000
5000
0
0.2
0.4
0.6
0.8
1.0
Export ratio (M/M0)
C
Decayed organic carbon content (mg C)
1.0
0.8
0.6
0.4
0.2
0
2
4
6
8
Salp cover (cm2)

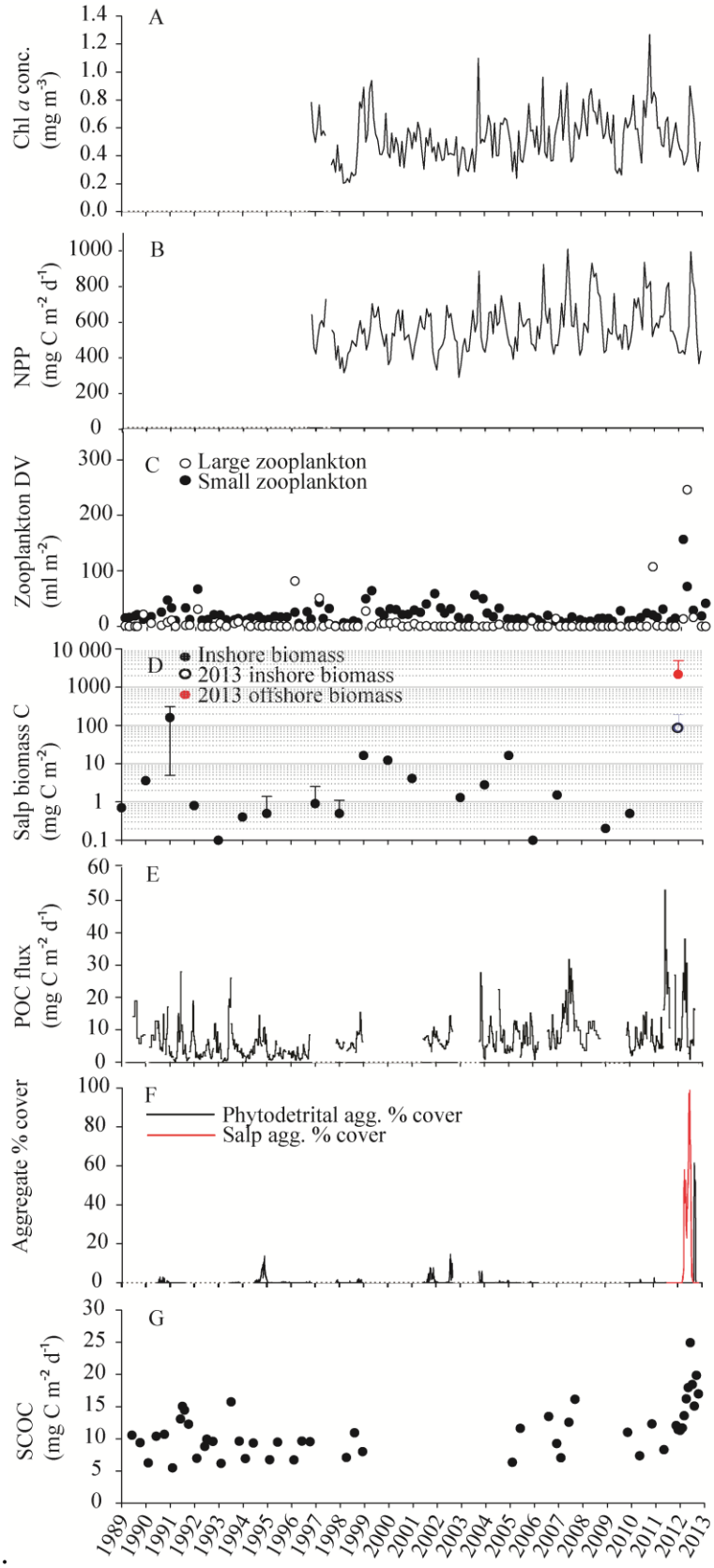
A
Chl a conc. (mg m-3)
1.4
1.2
1.0
0.8
0.6
0.4
0.2
0.0
B
NPP (mg C m-2 d-1)
1000
800
600
400
200
0
C
Large zooplankton
Small zooplankton
Zooplankton DV (ml m-2)
300
200
100
0
D
Inshore biomass
2013 inshore biomass
2013 offshore biomass
Salp biomass C (mg C m-2)
10 000
1000
100
10
1
0.1
E
POC flux (mg C m-2 d-1)
60
50
40
30
20
10
0
F
Phytodetrital agg. % cover
Salp agg. % cover
Aggregate % cover
100
80
60
40
20
0
G
SCOC (mg C m-2 d-1)
30
25
20
15
10
5
0
1989
1990
1991
1992
1993
1994
1995
1996
1997
1998
1999
2000
2001
2002
2003
2004
2005
2006
2007
2008
2009
2010
2011
2012
2013

705 Figure 2.

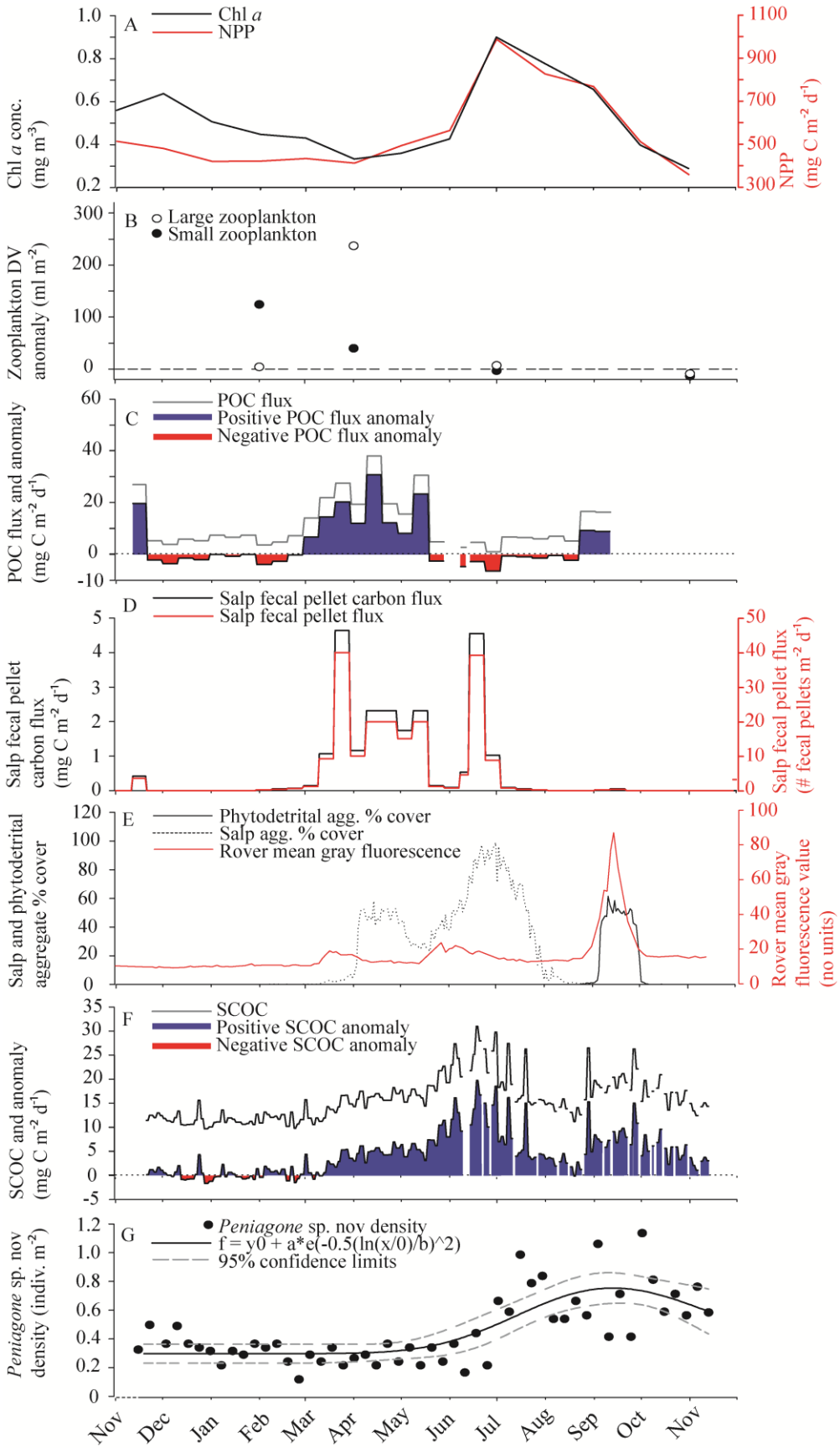
A
Chl a
NPP
Chl a conc. (mg m-3)
NPP (mg C m-2 d-1)
B
Large zooplankton
Small zooplankton
Zooplankton DV anomaly (ml m-2)
C
POC flux
Positive POC flux anomaly
Negative POC flux anomaly
POC flux and anomaly (mg C m-2 d-1)
D
Salp fecal pellet carbon flux
Salp fecal pellet flux
Salp fecal pellet carbon flux (mg C m-2 d-1)
Salp fecal pellet flux (# fecal pellets m-2 d-1)
E
Phytodetrital agg. % cover
Salp agg. % cover
Rover mean gray fluorescence
Salp and phytodetrital aggregate % cover
Rover mean gray fluorescence value (no units)
F
SCOC
Positive SCOC anomaly
Negative SCOC anomaly
SCOC and anomaly (mg C m-2 d-1)
G
Peniagone sp. nov density
f = y0 + a*e(-0.5(ln(x/0)/b)^2)
95% confidence limits
Peniagone sp. nov density (indiv. m-2)
Nov
Dec
Jan
Feb
Mar
Apr
May
Jun
Jul
Aug
Sep
Oct
Nov

706 Figure 3.

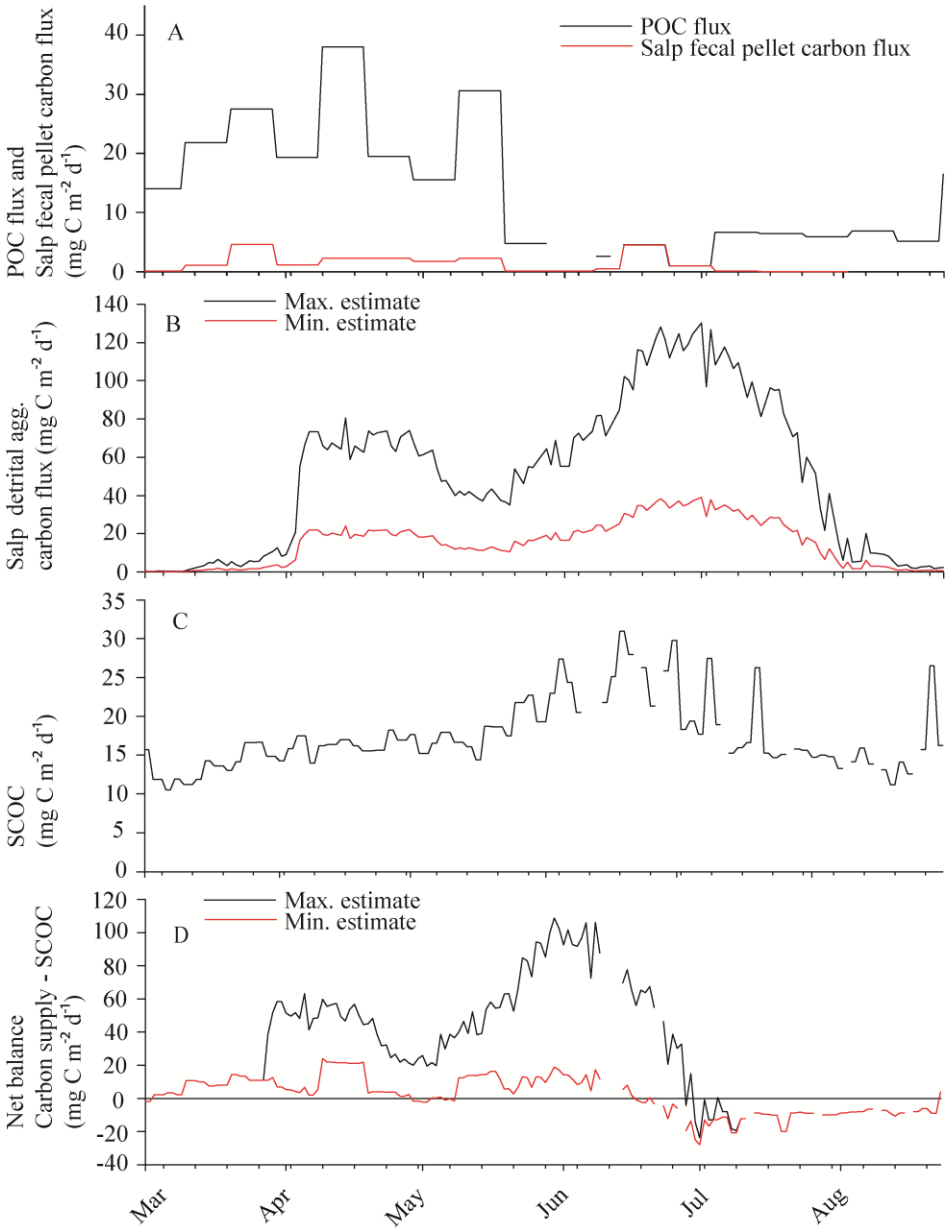

707

708 Figure 4.

709